Ultrasound holography for noninvasive imaging of buried defects and interfaces for advanced interconnect architectures

Gajendra Shekhawat,[1,a)] Arvind Srivastava,[1,2] Shraddha Avasthy,[2] and Vinayak Dravid[1,2,a)]
[1]*International Institute for Nanotechnology and the NUANCE Center, Northwestern University, Evanston, Illinois 60208, USA*
[2]*Department of Material Science and Engineering, Northwestern University, Evanston, Illinois 60208, USA*

(Received 5 August 2009; accepted 22 October 2009; published online 28 December 2009)

Imaging high resolution subsurface defects nondestructively in advanced interconnect structures and devices is a challenge and no known metrology tools are available to identify such defects in a nondestructive way at nanometer level. Monitoring these defects necessitate the understanding of their growth mechanism of these interconnects as well as defect formation. We report here the application of scanning near field ultrasound holography by imaging buried defects in copper interconnects and low-K dielectric materials. Defects in these copper lines such as voids and delaminations appear as regions of dark contrast in ultrasound holography imaging due to large acoustic impedance mismatch at the voids. Identification of these buried defects in these interconnect architectures in a nondestructive way will open up unique opportunities in using this technique to detect subsurface defects and material imperfections. © *2009 American Institute of Physics*. [doi:10.1063/1.3263716]

With rapid progress in the semiconductor device and interconnect technology, one of the important issues during the research and development phase of such technologies is the early identification of failures such as voiding, delaminations, cracks in interconnect structures and thermomechanical defects in low-K dielectric materials structures.

Due to the ever-increasing demands on performance, Al-based interconnects are now being replaced with Cu-based interconnects as they have many advantages such as low line resistance, low interconnect delay, high electromigration resistance and, possibly, overall back-end process simplicity. Some of the many challenges in the next generation metrology include dimensionality and fatigue performance of electrical contacts and interconnects.[1–5] Current paradigm for microelectronics electrical contact processing calls for an increase in the aspect ratio of metal contact lines which requires deposition of metal into damascene trenches and *vias* without leaving any unfilled volume (voids). These process defect voids result in increased resistivity and can cause serious open circuits and device failure. Conventional techniques for characterization of voids and incomplete contacts include destructive approaches such as cross-sectional scanning electron microscopy [or transmission electron microscopy (TEM)],[6] which are not only laborious and time consuming but require the wafer to be sacrificed. Electrical testing is nondestructive,[7] but spatially insensitive and it requires contact to the wafer.

Clearly, a need for nondestructive nanoscale high resolution imaging of buried and embedded structures in materials, devices, and pattern recognition is critical for numerous materials, structures, interconnect architectures and phenomena as they continue to shrink, and the micro/nanofabrication paradigm moves from planar to three-dimensional or stacked platforms.

The conventional approach for inspecting such failures nondestructively is scanning acoustic microscopy.[8–10] Ultrasound is sensitive to the presence of buried defects and these defects normally appear as regions of varying contrast in the image due to large acoustic impedance mismatch between the surrounding layer materials and the air. One of the main limitations of conventional acoustic microscopy is that the coupling medium, typically water, attenuates the ultrasound significantly at high frequencies. Scanning probe microscopy (SPM)[11–13] offers superb spatial resolution but is sensitive only to surface or shallow subsurface features. High resolution optical microscopy[14,15] is unable to image optically opaque or deeply buried structures. Thus, with respect to "nondestructive" imaging, there is a clear void between the two ranges of length-scales offered by photoacoustic/sonography[16–19] and SPM. This is particularly true if features of interest are buried deeper into the material, beyond the interaction range of proximal probes.

Several efforts combining SPM and acoustic methods for surface as well as subsurface imaging have been introduced in recent years with mixed results in the context of sensitivity to surface nanomechanical variations, ability to probe deeply buried or embedded features or quantitative extraction of nanomechanical contrast. Ultrasonic force microscopy and SPM based acoustic techniques[20–27] is notable SPM-based techniques which have enjoyed some success for nanomechanical mapping of elastic and viscoelastic properties of soft and hard surfaces. However, a wider deployment of these techniques in semiconductor applications is generally marred by lack of reproducibility and lack of compelling evidence for demonstrated sensitivity to buried and embedded structure. Our recent development for nanoscale imaging of buried nanostructures with high resolution using scanning near field ultrasound holography (SNFUH)[28–30] provides a very good technique for identifying and imaging buried defects and voiding in copper interconnects and low-K dielectric materials.

[a)]Authors to whom correspondence should be addressed. Electronic addresses: g-shekhawat@northwestern.edu and v-dravid@northwestern.edu.

 © 2009 American Institute of Physics

Downloaded 26 Oct 2010 to 133.28.47.30. Redistribution subject to AIP license or copyright; see http://apl.aip.org/about/rights_and_permissions

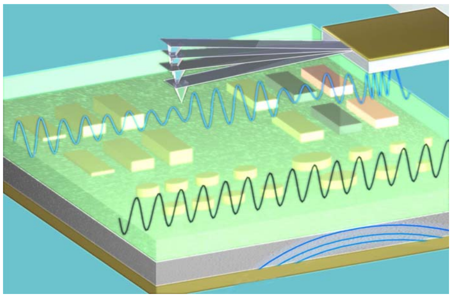

FIG. 1. (Color online) Schematic illustration of a copper interconnects lines. The thickness of the lines is around 500 nm. Cantilever detects the perturbations in the surface acoustic waves at the sample surface. The damping of the acoustic waves is higher at the void/defect site. Acoustic transducers underneath the sample and cantilever provide the ultrasonic waves through them.

In this article, we present SNFUH application for probing the buried defects and voiding in copper interconnect structures and sursurface mechanical imperfections in low-K dielectric material that overcome the fundamental problem of acoustic attenuation in the coupling medium by generating and detecting the subsurface perturbations directly at the sample surface with SPM probe as an acoustic antenna. The identified buried defects were cross-validated with dual beam focused ion-beam (FIB) microscope.

We have used JEOL SPM 5200 scanning probe microscope system with a modified stage and cantilever holder system to perform ultrasound holography. We have modified the feedback electronics of the system with a SNFUH electronic module along with lock-in amplifier to extract both the phase and amplitude of the surface acoustic waves perturbed by buried features. Commercial piezoelectric ceramics were used to provide ultrasonic vibrations to the sample and the cantilever, with an out-of-plane resonance of approximately 10.12 and 10.17 MHz, respectively.

The SNFUH controller and cantilever monitor the perturbation to the surface acoustic waves, especially their phase, which carry information about embedded structures reflected in the scattering of specimen acoustic waves due to the difference in their respective mechanical properties. Experimentally, the two acoustic oscillations are applied to the tip and the sample by two matching piezocrystals attached to the cantilever and at the base of the sample. Variations in the amplitude and phase of the bulk wave due to the presence of the subsurface nanostructures/defects as well as the variations in near surface affect the amplitude and the phase of the difference frequency signal which is detected by cantilever. These variations are used to create spatial mappings generated by subsurface and near-surface features/defects.

We here demonstrated the efficacy of SNFUH in identifying buried defects in copper interconnects. The sample comprises equally spaced interconnect copper lines fabricated by optical lithography. The thickness of these lines was around 500 nm. Figure 1 shows the schematic illustration of our model copper interconnect sample and the detection mechanism. Figure 2 shows a series of copper lines having thickness of around 500 nm. Figure 2(a) shows the conventional topography image, while Fig. 2(b) is the corresponding (simultaneously recorded) SNFUH phase image. The typical 25×25 μm^2 topography scan shows uniform and contiguous polymer and copper lines. However, the corresponding SNFUH *phase* image shown in Fig. 2(b) reveals

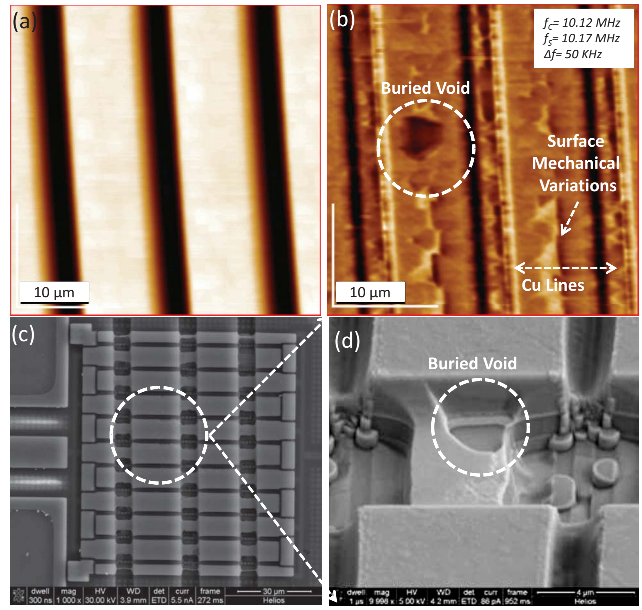

FIG. 2. (Color online) Schematic illustration of a copper interconnects lines. The thickness of the lines is around 500 nm. (a) shows the uniform topographical interconnect lines with some features visible. (b) shows the remarkable SNFUH phase image clearly demonstrates the voiding in these copper lines and other surface mechanical variations. (c) depicts the FIB image highlighting the area that was cut down to cross-validate the SNFUH image and (d) the cross section of one of the trench shows the buried defects when it was etched down from top by ion-milling.

phase contrast reminiscent of subsurface voiding in copper lines. The dark contrast in the phase image of copper lines corresponds to voids underneath the metal. The presence of this contrast in phase image implies that there is insufficient metal filling at the bottom, i.e., voiding underneath the contact, which undergoes a distinct viscoelastic response. Some of the topographical mechanical variations are also evident more prominently in the SNFUH image. These topographical variations originate from the chemical mechanical polishing of these interconnects lines. After SNFUH imaging, sample location was precisely marked and put down in FEI dual beam FIB to cross-validate what we got in ultrasound holography. Figure 2(c) depicts the planer view of the FIB image showing the area that we cut down to see the buried defects. Figure 2(d) depicts the FIB image of a defect found during SNFUH imaging. The lines were cut exactly at the same location where SNFUH was performed and the image clearly demonstrates the same buried defect that was found in ultrasound imaging. Thus, we validated the SNFUH buried imaging capabilities with FIB. These images clearly demonstrate the reliability of this method not only as a microscopy technique but also as an extremely sensitive probe of the mechanical reliability of the interfaces.

Recently, enormous amount of research is being carried out to fill shallow trenches with polymers to prevent extra processing steps. The trench isolation technique can be used to fabricate memory, logic and imager devices which can exhibit reduced current leakage and/or reduced optical crosstalk.

The major challenge that industry is facing with this technology is voiding, delamination and cracks at the polymer-trench interface. Conventional techniques for characterization of voids and stresses in narrower trenches include wet chemical etching and electrical testing, which is

Downloaded 26 Oct 2010 to 133.28.47.30. Redistribution subject to AIP license or copyright; see http://apl.aip.org/about/rights_and_permissions

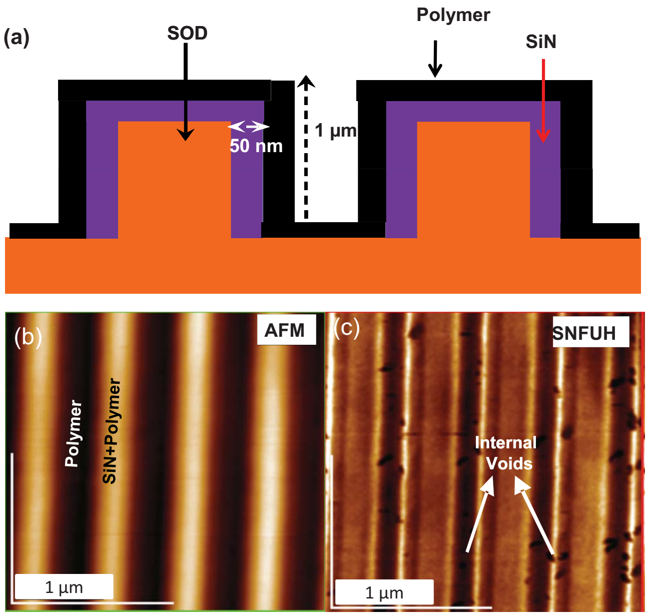

FIG. 3. (Color online) (A) Schematic of sample for detecting buried defects/voiding in shallow trenches. (B) Typical AFM topography image shows 500 nm thick coating of low dielectric material uniformly covering the trenches. Trench width is around 400 nm and height is about 1 μm having 500 nm BCB coating over it. (C) SNFUH image clearly reveals the surface elastic contrast and sub-surface voiding in polymer coating over silicon nitride (SiN).

spatially insensitive and it requires contact to the wafer. In the case of via chains, several metal levels must be fabricated before the electrical test can be completed. We demonstrated here underlying defects in narrower trenches by fabricating shallow trench structures as shown in Fig. 3(A). The trenches are etched in SOG (spin-on-dielectric) with a 50 nm thin layer of LPCVD (low pressure chemical vapor deposition) Si_3N_4 as a capping layer and then SiN (silicon nitride) is etched down in the trenches using the wet processing. Trenches were 1 μm deep. A 500 nm thick layer of polymer [benzocyclobutene (BCB)] was spin-coated followed by thermal annealing for curing polymer.

Schematic of series of isolated shallow trench structures having polymeric coating in them is shown in Fig. 3(a). Figure 3(b) depicts the conventional topography image, while Fig. 3(c) is the corresponding (simultaneously recorded) spectacular SNFUH phase image. The typical 2×2 μm^2 topography scan shows uniform and contiguous polymeric coating on SiN and inside the trenches. However, the corresponding SNFUH *phase* image shown in Fig. 2(c) reveals phase contrast reminiscent of buried voiding at the interface of the SiN/polymer or SiN/SOD. The dark contrast in the phase image on polymer coated SiN lines corresponds to voids at polymer-SiN /SiN-SOD interface. Interestingly, a hardening of the polymer in the trench and its sidewall is also evident in the phase image, which results from its thermal annealing and may be poor adhesion with SOG. These result demonstrates direct semiconductor metrology application of SNFUH system in recognizing buried patterns while maintaining high resolution.

In summary, the representative examples of SNFUH direct application in semiconductor structures and devices strongly suggest a versatile tool-set for nondestructive, high resolution and real-space imaging of diverse materials systems. Such a metrology capability opens up the possibility of high resolution failure and fatigue analysis to identify the buried defects, stress migration, cracks in semiconductor processing, devices and MEMS integration.

The SNFUH measurements were carried out in the NIFTI facility of NU*ANCE* Center at Northwestern University. NU*ANCE* Center is supported by the NSF-NSEC, NSF-MRSEC, Keck Foundation, the Station of Illinois, and Northwestern University. The research is supported by gift funding from Intel Corporation and NSF-MRI, SRC programs. The copper interconnect specimens were provided by Ted Liang, Intel Corporation.

[1]Y. B. Park, R. Monig, and C. A. Volkert, Thin Solid Films **504**, 321 (2006).
[2]J. Zhang, J. Y. Zhang, G. Liu, Y. Zhao, X. D. Ding, G. P. Zhang, and J. Sun, Scr. Mater. **60**, 228 (2009).
[3]M. Huang, Z. Suo, and Q. Ma, Acta Mater. **49**, 3039 (2001).
[4]R. R. Keler, R. Mönig, C. A. Volkert, E. Artz, R. Schwaiger, and O. Kraft, *Proceedings of the Sixth International Workshop on Stress-Induced Phenomenon in Metallization*, (American Institute of Physics, New York, 2002), p. 119.
[5]S. Moreau, S. Maitrejean, and G. Passemard, Microelectron. Eng. **84**, 2658 (2007).
[6]M. A. Meyer, M. Herrmann, E. Langer, and E. Zschech, Microelectron. Eng. **64**, 375 (2002).
[7]M. W. Cresswell, N. Aroara, R. A. Allen, C. E. Murabito, C. A. Ritcher, A. Gupta, L. W. Lingolm, D. Pa, and P. Bendix, Proceedings of the IEEE 2001 International Conference on Microelectronics Test Structures, 2001 (unpublished), Vol. 14, p. 183.
[8]G. A. D. Briggs, *An Introduction to Scanning Acoustic Microscopy* (Oxford University Press, Oxford, 1985).
[9]C. F. Quate, Phys. Today **38**, 34 (1985).
[10]E. Twerdowski, M. Buttlar, N. Razek, R. Wannemacher, A. Schindler, and W. Grill, Ultrasonics **44**, e1301 (2006).
[11]C. F. Quate. Surf. Sci. **299**, No. 1–3, 980 (1994).
[12]I. C. Gebeshuber, J. H. Kindt, J. B. Thompson, Y. Amo, H. Stachelberger, M. A. Brzezinsk, G. D. Stucky, D. E. Morese, and P. K. Hansma, J. Microsc. **212**, 292 (2003).
[13]G. S. Shekhawat, R. P. Gupta, S. S. Shekhawat, D. P. Runthala, K. B. Garg, and P. D. Vyas, Appl. Phys. Lett. **68**, 114 (1996).
[14]W. Dickson, S. Takahashi, R. Polland, and R. Atkinson, IEEE Trans. Nanotechnol. **4**, 229 (2005).
[15]M. Denyer, R. Micheletto, K. Nakajima, and M. Hara, J. Nanosci. Nanotechnol. **3**, 496 (2003).
[16]B. C. Larson, W. Yang, G. E. Ice, J. D. Budai, and J. Z. Tischler, Nature (London) **415**, 887 (2002).
[17]X. Wang, Y. Pang, G. Stoica, and W. Wang, Opt. Lett. **28**, 1739 (2003).
[18]K. P. Köstli and P. C. Beard, Appl. Opt. **42**, 1899 (2003).
[19]H. D. Zhong, J. B. Li, and Z. Sheng, Chinese Journal of Medical Imaging Technology **20**, 1815 (2004).
[20]L. Muthuswami and R. Geer, Appl. Phys. Lett. **84**, 5082 (2004).
[21]R. E. Geer, O. V. Kolosov, G. A. D. Briggs, and G. S. Shekhawat, J. Appl. Phys. **91**, 4549 (2002).
[22]Y. Zheng, R. E. Geer, K. Dovidenko, M. Kopycinska-Müller, and D. C. Hurley, J. Appl. Phys. **100**, 124308 (2006).
[23]O. V. Kolosov, M. R. Castell, C. D. Marsh, and G. A. D. Briggs, Phys. Rev. Lett. **81**, 1046 (1998).
[24]M. T. Cuberes, H. E. Alexander, G. A. D. Briggs, and O. V. Kolosov, J. Phys. D: Appl. Phys. **33**, 2347 (2000).
[25]M. Kopycinska-Müller, R. H. Geiss, J. Müller, and D. C. Hurley, Nanotechnology **16**, 703 (2005).
[26]K. B. Crozier, G. G. Yaralioglu, F. L. Degertekin, J. D. Adams, S. C. Minne, and C. F. Quate, Appl. Phys. Lett. **76**, 1950 (2000).
[27]H. R. Zeng, H. F. Yu, S. Hui, R. Q. Chu, and G. R. Li, Solid State Commun. **133**, 521 (2005).
[28]G. S. Shekhawat and V. P. Dravid, Science **310**, 89 (2005).
[29]L. Tetard, A. Passian, R. Lynch, G. Shekhawat, V. Dravid, and T. Thundat, Appl. Phys. Lett. **93**, 133113 (2008).
[30]L. Tetard, A. Passian, K. Venmar, R. Lynch, G. Shekhawat, V. Dravid, and T. Thundat, Nat. Nanotechnol. **3**, 501 (2008).

Downloaded 26 Oct 2010 to 133.28.47.30. Redistribution subject to AIP license or copyright; see http://apl.aip.org/about/rights_and_permissions